Applied Catalysis B: Environmental 180 (2016) 113–120

Contents lists available at ScienceDirect

Applied Catalysis B: Environmental

journal homepage: www.elsevier.com/locate/apcatb

Vapor phase hydrogenation of aqueous levulinic acid over hydroxyapatite supported metal (M = Pd, Pt, Ru, Cu, Ni) catalysts.

M. Sudhakar[a], V. Vijay Kumar[a], G. Naresh[a,b], M. Lakshmi Kantam[a], S.K. Bhargava[b], A. Venugopal[a,*]

[a] Inorganic and Physical Chemistry Division, Indian Institute of Chemical Technology, Uppal Road, Hyderabad, Telangana 500007, India
[b] Centre for Advanced Materials & Industrial Chemistry (CAMIC), School of Applied Sciences, RMIT University, GPO BOX 2476,Melbourne 3001, Australia

ARTICLE INFO

Article history:
Received 12 December 2014
Received in revised form 28 April 2015
Accepted 26 May 2015
Available online 9 June 2015

Keywords:
Levulinic acid
Gamma-valerolactone
Hydroxyapatite
Ru
Nh_3-tpd
Co_2-tpd
TEM

ABSTRACT

$Ca_5(PO_4)_3(OH)$ (HAP) supported metal (Ru, Pt, Pd, Cu and Ni) catalysts were examined for vapour phase hydrogenation of aqueous levulinic acid (LA). Ru/HAP demonstrated higher TOF of γ-valerolactone (gVL) over the other metal catalysts. The LA dehydration products such as angelica lactones (both α- and β-AL) were formed significantly over Pt, Pd, Ni and Cu/HAP catalysts. Influence of Bronsted and Lewis acid sites was exemplified by pyridine adsorbed FT-IR studies on Ru/HAP that exhibited very weak band due to Bronsted sites at 1552 cm^{-1} and a strong band at 1450 cm^{-1} attributed to Lewis acid sites. Ru supported on SO_4^{2-}-HAP demonstrated selective dehydration of LA to α-angelica lactone. Hydrogenation activity of Ru was diminished while supported on SO_4^{2-} -HAP, quite contrast to this the fresh HAP behaved as a selective support for Ru towards GVL formation. Thus, HAP has been identified as suitable support for Ru in the conversion of LA at ambient pressure.

1. Introduction

The present imbalance in the demand-supply scenario of fuels and chemicals from fossil fuel resources with an increased consumption and rapid depletion of these led the R&D to focus on renewable (infinite) resources such as lignocellulose to provide alternatives to conventional fuels [1–4]. Liquid bio-fuels derived from the renewable plant mass are better options to be considered for the existing fuel sources. Levulinic acid (LA) is regarded as an important bio-based platform chemical that can be easily and cheaply produced by a simple hydrolysis of lignocellulose [5,6]. γ-valerolactone (gVL) an intermediate compound for various solvents, chemicals and a blending agent in fuels is synthesized by hydrogenation of levulinic acid [7–13]. Hence, synthesis of gVL from LA has attracted greater attention of researchers around the world.

Several homogeneous catalysts were explored for the conversion of levulinic acid to γ-valerolactone [14,15]. However, the heterogeneous catalytic processes are more economical as they offer advantages such as ease of recovery and recycling [16,17]. There are few reports on the vapour phase hydrogenation of levulinic acid at atmospheric pressure. Recently, Upare et al. reported 98.6% yield of γ-valerolactone over Ru/C catalyst using dioxane as a solvent at high H_2 pressures [18]. Earlier we have shown a gVL rate of 15 mol h^{-1} $(mol_{Ru})^{-1}$ at moderate temperature over Ru/HAP at 5 bar H_2 pressure [19]. The high hydrogenation activity of Ru/HAP has prompted us to explore it further at ambient pressure for the conversion of LA to gVL. The criteria for choosing metal (Pt, Pd, Ru, Ni and Cu) supported on HAP catalysts are: (i) Hydroxyapatite can be a good support for several catalytic processes owing to its porous nature and for possessing both acidic and basic sites. (ii) HAP has been exploited as a support material for hydrogenation reactions [20]. (iii) HAP is a stable support under hot carboxylic acid (i.e., LA) unlike other conventional supports such as alumina and MgO [21]. (iv) It has also been explored as a catalyst support for gold and ruthenium in the water gas shift reaction as well as a stand-alone catalyst for the dehydrogenation and dehydration of alcohols [22–25]. In the present study, LA hydrogenation has been carried out under kinetic regime at atmosphere pressure in the temperature range of 275–425 °C. The reaction pathway from LA to gVL is dependent upon the catalyst acidity and hydrogenation activity of metal [19]. The multiple pathways reported are: (i) hydrogenation of LA via γ-hydroxyvaleric acid, as an intermediate compound in equilibrium with gVL and (ii). dehydration of LA to form angelica lactone followed by its hydrogenation to pro-

* Corresponding author. Fax: +91 40 27160921.
E-mail address: akula@iict.res.in (A. Venugopal).

http://dx.doi.org/10.1016/j.apcatb.2015.05.050
0926-3373/

duce gVL. Recently some of the important findings were reported by Dumesic group and Weckhuysen and co-workers on the levulinic acid conversion to valeric biofuels and fuel additives [26–28]. In parenthesis developemnt of catalysts for the hydrodeoxygenation (HDO) of biomass derived acids in to hydrocarbons is gaining momentum. In a study Yuliana et al. reported the gas-phase HDO of propanoic acid to ethane and propane over Ru/SiO_2 catalyst at very moderate temperatures and ambient H_2 pressure [29]. A detailed kinetic studies on hydrocracking and HDO of biomass derived compounds using hydrogen donor solvents is established by Grilc et al. over several Ni and Pd based catalysts [30–32].

Dumesic et al. reported that rate of gVL is dependent on the nature and strength of acid sites present on the catalyst [9]. Kon et al. distinguished the effect of Bronsted and Lewis acid sites on the ring opening of gVL to pentanoic acid [33]. The acid sites on catalyst surface seem to play an important role in the conversion of LA into gVL [34]. We thus focussed our studies on influence of acid sites (Bronsted and/or Lewis) on dehydration of LA as well as on ring opening of gVL to hydroxyvaleric acid (HVA) which is examined by FT-IR analysis of pyridine adsorbed Ru/HAP catalysts. An insight on the role of catalyst acidity in the ring opening of gVL and also dehydration of LA is gained by enhancing the surface acidity through impregnation of SO_4^{2-} on HAP (SO_4^{2-}-HAP) and subsequent deposition of 2 wt% of Ru on SO_4^{2-}-HAP followed by calcination in N_2 at 450 °C /3 h. The LA conversion rate on Ru/SO_4^{2-}-HAP has been compared with Ru/HAP catalyst under identical experimental conditions. Ru/HAP did not show any ring opening activity even with the presence of very weak surface hydroxyl groups on the surface that resulted in >99% selectivity to gVL. We have also observed that the moderate Lewis acid sites are responsible for dehydration of LA at high reaction temperatures to produce angelica lactones over Ru/HAP.

The catalyst samples were characterized by BET-surface area, transmission electron microscope (TEM), temperature programmed desorption (TPD of NH_3 and TPD of CO_2), temperature programmed reduction (TPR), X-ray photoelectron spectroscopy (XPS), carbon hydrogen, nitrogen and sulphur (CHNS) analysis and CO pulse chemisorption studies for the measurement of metal dispersion. Role of Bronsted and Lewis acid sites is explained based on pyridine adsorbed FT-IR spectroscopy.

2. Experimental

2.1. Preparation of catalysts

The hydroxyapatite ($Ca_5(PO_4)_3(OH)$) was prepared according to an earlier report in the literature [22]. In a typical method, the solution of calcium nitrate tetrahydrate (0.326 mol) in 200 mL water was brought to a pH of 11–12 with concentrated (25%) ammonia solution and thereafter diluted to 500 mL. A solution of diammonium hydrogen phosphate (0.318 mol) in 300 mL water was brought to a pH of 11–12 with concentrated (25%) ammonia solution and thereafter diluted to 600 mL. Under vigorous stirring the phosphate solution was added drop wise to the solution of the calcium salt over a period of 2 h to produce a milky white precipitate, which was then stirred and boiled for 30 min. The precipitate was washed thoroughly, filtered and dried at 100 °C over night and then calcined in static air at 500 °C for 5 h. The HAP supported metal catalysts were prepared by a wet impregnation method. The required amount of metal precursor [($RuCl_3$ xH_2O, $PdCl_2$, H_2PtCl_6 $6H_2O$, $Cu(NO_3)_2$ $3H_2O$ and $Ni(NO_3)_2$ $6H_2O$) AR Grade, supplied by Sigma–Aldrich] was taken to give metal loading of 2 and/or 5 wt% over HAP. The solvent is then evaporated with constant stirring. The samples were dried at 120 °C for 12 h and subsequently calcined in air at 450 °C for 5 h at a ramping rate of 5 °C/min. The sulphated HAP support was prepared by the immersion of about 0.95 g of HAP in 30 mL of 0.5 M H_2SO_4 under vigorous stirring for 3 h at ambient temperature. Excess water was evaporated on a water bath and the resulting sample was oven dried at 100 °C, followed by calcination in air at 450 °C for 3 h to obtain the sulphated HAP. The 2 wt% Ru/sulphated HAP sample was prepared by impregnation method. In a typical method required amount of ruthenium chloride hydrate ($RuCl_3$ xH_2O) was mixed with calcined sulphated HAP. The solution was stirred at 100 °C until the sample gets dried and then kept for drying over night at 100 °C, followed by calcination in static air at 450 °C for 3 h.

2.2. Vapor phase hydrogenation of aqueous levulinic acid

Vapor phase hydrogenation of aqueous levulinic acid (LA) was carried out over calcined metal (M = Pt, Pd, Ru, Ni and Cu) supported on hydroxyapatite catalysts in a fixed-bed down flow quartz tubular reactor (i.d. = 12 mm, length = 450 mm) at atmospheric pressure. The reactor was packed with ≈0.250 g catalyst. The catalyst was reductively pre-treated in H_2 at 450 °C for 3 h prior to the reaction. Aqueous levulinic acid (or otherwise in CH_3OH and/or C_2H_5OH) was fed (using a calibrated feed pump) at a flow rate of 1 and/or 2 mL h^{-1} along with H_2 at a flow rate = 20 mL min^{-1}. The reaction was performed in the temperature range of 275–425 °C. The products were collected in an ice-bath at regular intervals and analyzed by gas chromatograph (Shimadzu, GC-17A) via a flame ionization detector (FID) using a ZB-5 capillary column at a ramping rate of 10 °C min^{-1} from 60 to 280 °C. The carbon mass balance in all the measurements was >98% even after 48 h of continuous operation. The samples were analyzed by GC–MS (QP5050A Shimadzu) using a ZB-5 capillary column with EI mode.

$$\text{Conversion of LA}=\left(\frac{\text{LAc}_{\text{in}}-\text{LAc}_{\text{out}}}{\text{LAc}_{\text{in}}}\right)\times 100$$

$$\%\text{Selectivity}=\frac{\text{pi/ci}}{\Sigma_i^n \text{pi/ci}}\times 100$$

(where ci and Pi are the stochiometric factor and the product concentration, respectively).

$$\text{Yield}=\frac{(\text{Conv. of LA})\times(\text{Sel. of GVL})}{100}$$

$$\text{Rate}=\frac{(\text{Yield})\times(\text{LA feed rate})}{(\text{weight of catalyst})}$$

$$\text{TOF}=\frac{\text{Rate}}{\text{CO uptake}}$$

2.3. Characterization of catalysts

The surface properties of both fresh and reduced samples were measured by N_2 adsorption at −196 °C, in an Autosorb 3000 physical adsorption apparatus. The specific surface areas were calculated applying the BET method. TPD of NH_3 and TPD of CO_2 was carried out using an Auto Chem 2910 (Micromeritics, USA). The amount of desorbed NH_3 and CO_2 was calculated using GRAMS/32 software. TPR analysis was carried out in a quartz micro-reactor interfaced to a GC equipped with a TCD unit. Hydrogen consumption was measured by analyzing effluent gas using a calibration curve of TPR of Ag_2O under a similar protocol. The carbon contents of the used samples were measured using a VARIO EL, CHNS analyser. The reduced and used catalysts were characterized by powder XRD analysis using a Rigaku Miniflex X-ray diffractometer using Ni filtered Cu Kα radiation (λ = 0.15406 nm) from 2θ = 20°–80°, at a scan rate of

Table 1
Physicochemical characteristics of HAP supported metal (M = Pt, Pd, Ru, Cu and Ni) catalysts.

Catalyst	Surface area (m^2/g)	H_2 uptake (μmol/g)[a]	CO uptake (μmol/g)	Dispersion (%)[b]	Metal area (m^2/g)[c]	Particle Size (nm)[d]	Carbon (wt.%)[e]
HAP	48.7	–	–	–	–	–	–
2wt.%Pd/HAP	36.5	124.2	36.4	19.3	1.7	6.19	1.3
2wt.%Pt/HAP	34.3	86.3	28.8	28.1	1.3	4.30	1.8
2wt.%Ru/HAP	39.4	79.8	30.6	15.4	1.5	7.44	0.3
5wt.%Ni/HAP	31.0	246.5	67.2	7.9	8.9	3.75	0.9
5wt.%Cu/HAP	35.8	206.7	nd	–	–	–	2.3

nd: not determined.
[a] H_2 uptakes measured by TPR analysis calibrated with TPR of Ag_2O.
[b] %Dispersion = [CO uptake (μmol/g_{cat}) × 100] / [total metal (μmol/g_{cat})].
[c] Metal area = metal cross sectional area × No. of metal atoms on surface.
[d] Particle size (nm) = 6000/[metal area (m^2 g M^{-1}) × ρ]; ρ: metal density.
[e] The carbon contents on the used catalysts recovered after 6 h.

2° min^{-1} with generator voltage and current of 30 kV and 15 mA respectively. The XPS patterns were recorded using a Kratos Axis Ultra Imaging X-ray photoelectron spectrometer, equipped with Mg anode and a multichannel detector. Charge referencing was done against adventitious carbon (C 1s, 284.8 eV). A Shirley-type background was subtracted from the signals. The recorded spectra were fitted using Gauss–Lorentz curves to determine the binding energies of the different elements. The morphological analysis was carried out using transmission electron microscopy (TEM on a JEOL 100S microscope at high resolution (HR) on a JEOL 2010 microscope). The samples were collected after 6 h on stream and analysed by GC (Varian GC-2010 FID) equipped with ZB5 wax capilliary column and GC–MS-QP-5050 (M/s. Shimadzu Instruments, Japan). CO pulse chemisorption was studied using an online gas chromatograph equipped with a thermal conductivity detector (TCD). Prior to analysis, the pretreatment of the catalyst was done using helium at 200 °C. The catalyst samples were reduced in H_2 flow (50 mL min^{-1}) at 450 °C for 3 h with a heating rate of 10 °C /min. Subsequently, the sample was purged with helium for 20 min and finally cooled down to 50 °C. CO was pulsed at 50 °C over the reduced catalyst and the amount of CO consumed was determined from the GC-TCD analysis. The nature and strength of acid sites on Ru/HAP, Ru/TiO_2 and Ru/SO_4^{2-}-HAP samples were analysed by FT-IR (Carry 660, Agilent Technologies) spectra in the range of 1800–1300 cm^{-1} with a resolution of 4 cm^{-1} and 64 scans. The spectra were collected *in- situ* using a purpose-made IR cell connected to a conventional vacuum-adsorption apparatus. The sample powders were pressed into self-supporting wafers (density~40 mg/cm^2) under a pressure of 10^5 Pa and then introduced into the IR cell. Successive treatments given prior to the analysis were: (i) the samples were reduced *in-situ* by heating in H_2/Ar flow (5 mL min^{-1}) at a ramping rate of 10 °C/min up to 450 °C/1 h. (ii) After cooling down to 150 °C the spectra were collected in the DRIFT mode. (iii) Subsequently the samples were exposed to steam at 275 °C and then flushed in N_2 (5 mL min^{-1}) for 30 min followed by the recording of spectra. (iv) In sequential step the samples were cooled to 180 °C and doses of pyridine were injected and the spectra were recorded. The *drift* spectra after pyridine adsorption were subtracted with that of spectra recorded in step (iii) in order to obtain the vibrational bands due to pyridine adsorption on the catalyst surface. Finally, the spectra were quantified with Kubelka-Munk function.

3. Results

3.1. Temperature programmed reduction (TPR)

The reduction behavior of HAP supported metal (M = Pt, Pd, Ru, Ni and Cu) catalysts analysed by TPR (Fig. 1) and the H_2 uptakes are reported in Table 1. TPR pattern of Pd/HAP catalyst showed a reduction signal centered at T_{max} ~ 208 °C (Fig. 1a). The Cu/HAP sample showed a large reduction peak centered around 237 °C (Fig. 1b). These reduction signals are assigned to PdO and CuO species respectively. In case of Ru/HAP one broad peak at 338 °C with shoulder at 440 °C is observed. The high temperature peak is linked to a very stable Ru species assigned to its oxychloride and the low temperature peak to Ru cations well dispersed at the surface (Fig. 1c) [35]. Pt/HAP exhibited a broad reduction maxima at 360 °C (Fig. 1d). A broad reduction signal shown by Ni/HAP (Fig. 1e) at 429 °C is due to the NiO particles in interaction with HAP.

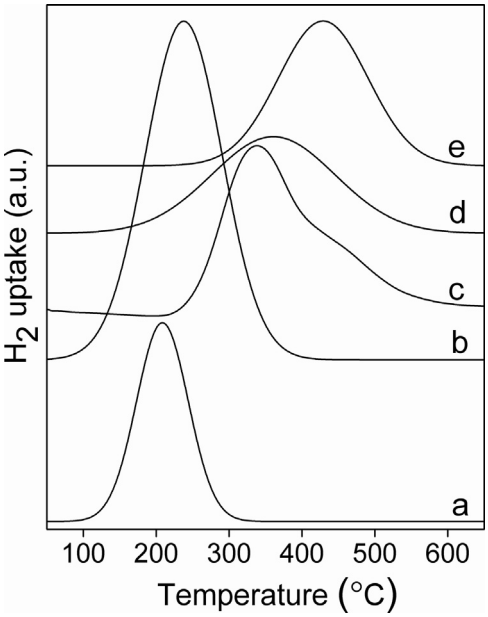

Fig. 1. TPR patterns of (a). 2 wt.%Pd, (b). 5 wt.%Cu, (c). 2 wt.%Ru, (d). 2 wt.%Pt and (e). 5 wt.%Ni supported on $Ca_5(PO_4)_3(OH)$ catalysts.

3.2. X-ray photoelectron spectra (XPS)

In order to understand the surface characteristics and to ensure the role of metallic species which is a pre-requisite for the hydrogenation of LA; the samples of Ru, Pt, Pd, Cu and Ni supported on HAP in reduced (in 5%H_2/Ar at 450 °C/3 h) form are subjected to XPS analysis (Fig. 2). The Ru/HAP (Fig. 2a) demonstrated a signal at binding energy (BE) of 280.5 eV assigned to Ru $3d_{5/2}$ which is an indication of Ru (0) in the near surface region [36]. The peak that appeared (Fig. 2b) at a BE of 335.7 eV is ascribed to metallic Pd (Pd $3d_{5/2}$) in Pd/HAP [36]. The Pt 4f signal located at 71.42–71.57 eV in Pt/HAP (Fig. 2c) sample, is a characteristic of Pt(0) [37]. The BE values of Ni $2p_{3/2}$ and Ni $2p_{1/2}$ peaks are observed around 852.9 and 871.1 eV respectively (Fig. 2d) [38]. Binding energy value of

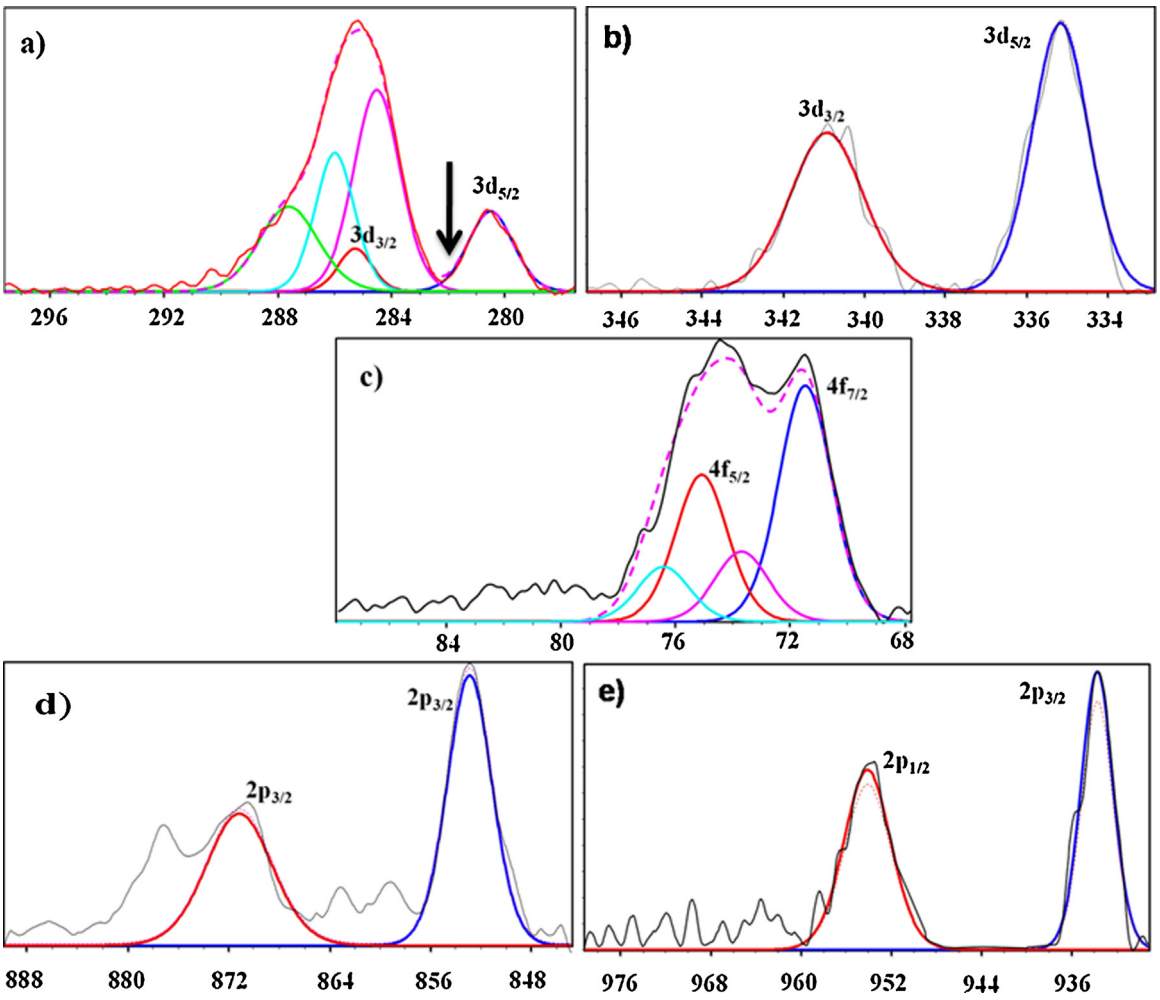

Fig. 2. XPS analysis of (a) Ru 3d, (b) Pd 3d, (c) Pt 4f, (d) Ni 2p and (e) Cu 2p spectra.

metallic Cu (Fig. 2e) is observed at 932.65 eV on Cu/HAP [39]. All the samples (M = Pt, Pd, Ru, Ni and Cu) M/HAP exhibited metallic species at the near surface region.

3.3. Carbon monoxide chemisorption and BET surface area measurements

The BET surface area of HAP and metal (M = Pt, Pd, Ru, Ni and Cu) M/HAP catalysts are reported in Table 1. A decrease in surface area is observed with supported metal catalysts when compared to pure HAP. The number of surface metal sites is assumed to be equal to the number of CO moles adsorbed on catalyst surface. The CO uptakes of metal/HAP (Metal = Pt, Pd, Ru, Ni and Cu) catalysts are in the following order: Ni > Pd > Ru > Pt.

3.4. Activity measurements on metal supported on hydroxyapatite catalysts

The vapour phase hydrogenation of aqueous levulinic acid is examined over Pt, Pd, Ru, Ni and Cu supported on hydroxyapatite at ambient pressure and the data is reported in Table 2. Under identical conditions, Ru exhibited better performance with respect to LA conversion and gVL selectivity. In the comparative analysis the turnover frequency (TOF) of gVL is higher with Ru/HAP ($\sim$2.9 s^{-1}) than other metal catalysts. The gVL turnover rate on Pt/HAP catalyst is higher than Ni/HAP by an order of magnitude. The Pt/HAP demonstrated good gVL yields with appreciable amount of angelica lactones (AL). Except Ru, all the metals have shown significant amount of α- and/or β-angelica lactones (>20%). Amount of α-angelica lactone is found to be greater than its β-form. The Ru/HAP showed better gVL rate than Pd and Pt although the metal dispersion (Table 1) is lower, suggests its high intrinsic activity in the selective hydrogenation of LA. The rate of gVL over the metal catalysts is in the following order: Ru > Pt > Cu > Pd > Ni/HAP. Based on this preliminary data the Ru/HAP catalyst has been further explored in order to investigate its intrinsic property for the selective hydrogenation of LA to gVL.

3.5. Characterization of Ru/HAP catalyst

XRD patterns of HAP, both calcined and reduced form of 2 wt.% Ru/HAP samples revealed the presence of $Ca_5(PO_4)_3(OH)$ phase alone (SI). The diffraction lines at $2\theta = 25.8^\circ$, 29.1°, 31.9°, 32.2°, 33.1°, 34.1°, 40.1°, 46.9°, 49.1° and their corresponding '*d*' values 0.344, 0.306, 0.279, 0.277, 0.269, 0.262, 0.224, 0.193, 0.183 nm [ICDD # 86-07640] are attributed to $Ca_5(PO_4)_3(OH)$ phase [22]. No peaks corresponding to either oxidic or metallic-Ru phases are found, thus suggesting a finely distributed nano sized Ru particles on HAP surface.

The TEM images of fresh, reduced and used Ru/HAP catalysts are shown in Fig. 3. Ru nanoparticles are more or less in spherical shape and found to be with a mean diameter in the range of 7–9 nm as seen in fresh Ru/HAP (Fig. 3a). The average Ru particle size increased (10–16 nm) in reduced and compared to its fresh form (Fig. 3b and

Table 2
Hydrogenation of aqueous levulinic acid over HAP supported metal (M = Pt, Pd, Ru, Cu and Ni) catalysts; GHSV = 2.616 mL g_{cat}^{-1} s^{-1} at a reaction temperature of 275 °C.

Metal (wt.%)/HAP	LA Conversion(mol%)	Selectivity (mol%)			r_{GVL}	$TOF_{GVL}(s^{-1})$
		GVL	β-AL	α-AL		
2Pd	25.3	66.5	12.5	21.0	16.2	0.44
2Pt	88.2	78.6	4.2	17.1	66.9	2.32
2Ru	92.2	99.8	0.0	0.2	88.8	2.90
5Ni	21.0	65.0	12.8	22.2	13.1	0.19
5Cu	32.2	74.8	9.6	15.6	23.2	–

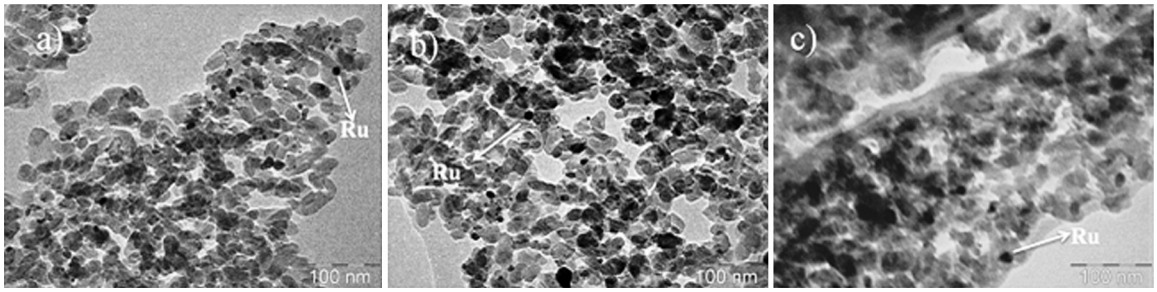

Fig. 3. TEM analysis of 2 wt.%Ru/ $Ca_5(PO_4)_3(OH)$ (a) Fresh and (b) Reduced (c) Used catalysts.

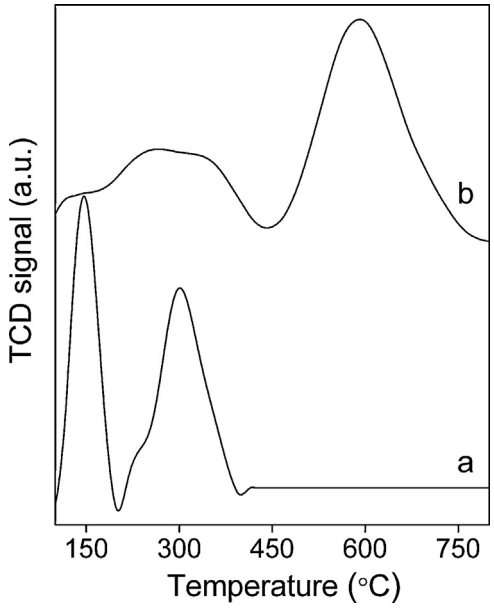

Fig. 4. TPD of CO_2 patterns of (a) $Ca_5(PO_4)_3(OH)$ and (b) 2 wt.%Ru/$Ca_5(PO_4)_3(OH)$ samples.

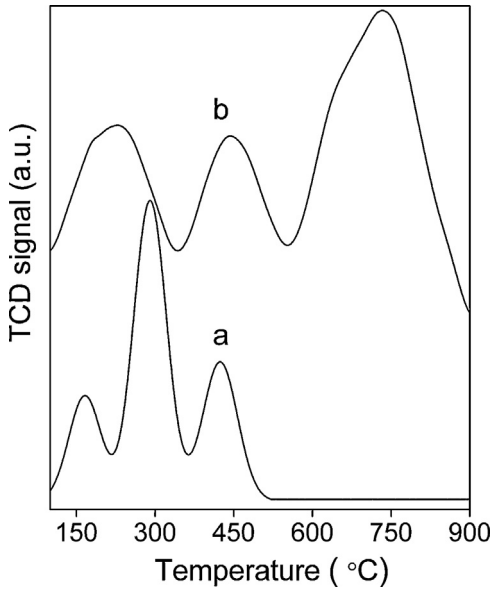

Fig. 5. TPD of NH_3 patterns of (a) $Ca_5(PO_4)_3(OH)$ and (b) 2 wt.%Ru/$Ca_5(PO_4)_3(OH)$ samples.

Table 3
Acid-base strength of hydroxyapatite and Ru supported on hydroxyapatite.

Catalyst	BET-surface area(m^2/g)	uptake (μmol/m^2)	
		NH_3	CO_2
HAP	48.0	0.28	0.27
Ru/HAP	39.4	1.14	0.24
Ru/SO_4^{2-} - HAP	32.8	7.12	nd

nd: not determined.

c). The enlargement of Ru particles seems to have happened during the reduction process. This observation is close to the Ru particle size measured from CO uptake that showed about 7.4 nm (Table 1).

The CO_2-TPD patterns of HAP and Ru/HAP samples are shown in Fig. 4 and the CO_2 uptakes are reported in Table 3. The desorption profiles indicated the presence of both weak and moderate basic sites on HAP surface. CO_2 desorption on HAP support is completed below 400 °C, with a sharp peak at 150 °C corresponding to weak basic sites and second one at 300 °C, assigned to moderate basic sites. On the other hand, the Ru/HAP exhibited a small but broad CO_2 desorption peak below 400 °C and an intense peak centred at 590 °C. Addition of Ru to HAP, resulted in the decrease in weak and moderate basic sites with a corresponding increment of strong basic sites where a strong CO_2 desorption peak is found at 590 °C, although the total CO_2 uptake is less on Ru/HAP (Table 3).

The NH_3-TPD patterns of HAP and Ru/HAP samples are presented in Fig. 5. HAP showed complete desorption of NH_3 below 500 °C with three sharp peaks centred at T_{max} of 150°, 280° and 425 °C. These peaks are assigned to very weak and two moderate acid sites respectively. In case of Ru/HAP, NH_3 desorption peaks appeared at 200°, 450° and 750 °C, which are attributed to weak, moderate and strong acidic sites.

The TPD of CO_2 and TPD of NH_3 studies demonstrated the presence of both acidic and basic sites on the Ru/HAP surface. Deposition

Table 4
Effect of reaction temperature on hydrogenation of aqueous levulinic acid over 2 wt% Ru/HAP; GHSV = 3.89 mL g_{cat}^{-1} s^{-1}.

Temperature(°C)	LA conversion(mol%)	Selectivity (mol%)		
		GVL	β-AL	α-AL
275	65.1	99.8	–	–
325	76.5	92.6	2.4	5.0
375	87.9	84.0	4.8	12.2
425	94.0	80.5	5.5	13.0
[a]275	4.0	0.0	0.0	100
[b]275	44.5	4.2	0.0	92.8
		[c]3.0		

[a] Activity using pure levulinic acid at GHSV = 2.616 mL g_{cat}^{-1} s^{-1}.
[b] Activity data on Ru/SO_4^{2-} - HAP catalyst at GHSV = 2.616 mL g_{cat}^{-1} s^{-1}.
[c] %Selectivity of pentanoic acid.

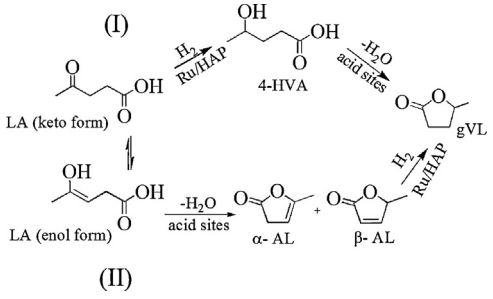

Scheme 1. Possible reaction pathways in the conversion of LA to gVL.

of $RuCl_3.xH_2O$ on HAP (Ru/HAP), resulted in the increase of acidity by four times and 10% decrease in the basicity compared to HAP (Table 3). The enhanced acidity of Ru/HAP may probably be due to traces of chloride moiety present on the catalyst [19]. The FT-IR spectra (SI, Fig. S4) of pyridine adsorbed Ru/HAP sample further confirmed the increase Lewis acidity of the catalyst. However, there is no changes in the Bronsted acidity while compared to HAP.

4. Discussion

Hydrogenation of LA is carried out over Ru/HAP at various reaction temperatures in the range 275–425 °C at a GHSV = 3.89 mL g^{-1} s^{-1} and the results are reported in Table 4. With increase in reaction temperature, the conversion of LA increased from 65 to 94%. However, selectivity of gVL decreased from 99.8 to 80% by the formation of both α- and/or β-angelica lactones at the cost of gVL as no by-products other than these angelica lactones are observed at all temperatures. We believe that at high reaction temperatures the moderate acid sites may be involved in the conversion of LA to angelica lactones. Based on the product distribution a plausible mechanism is proposed (Scheme 1). The mechanism follows in two pathways, one by hydrogenation of LA to 4-hydroxyvaleric acid; secondly the enol form of LA is undergoing dehydration to form angelica lactone. According to which at low reaction temperature, levulinic acid undergoes hydrogenation to form 4-hydroxyvaleric acid, subsequently transformed to γ-valerolactone by dehydration reaction. In contrast at high reaction temperatures, dehydration of levulinic acid seems to occur in parallel to hydrogenation to form angelica lactone. Another possibility is that the formed angelica lactone may subsequently undergo hydrogenation into γ-valerolactone (Scheme 1).

At moderate reaction temperatures both hydrogenation and dehydration of LA occur where as at high temperatures, dehydration of LA is slightly higher (Table 4). However, based on the product distribution it can be concluded that the rate of hydrogenation of LA is higher than the rate of dehydration. Contrary to this, rate of dehydration of LA is high as large amount of AL is observed at high temperatures. These results thus suggest the importance of acid functionality in the conversion of LA on Ru/HAP catalyst.

Formation of gVL occurred by simultaneous hydrogenation and dehydration reaction and conversely dehydration followed by hydrogenation thus also produce gVL. The Ru/HAP exhibited high temperature NH_3 desorption peak attributed to strong acid sites (Table 3). Therefore these strong acid sites (Fig. 5) seem to be involved at high reaction temperatures to some extent that initiate the reaction via dehydration of LA to produce AL. If the hydrogenation and dehydration reactions occur at similar rate, one would expect equal proportions of gVL and AL. Nevertheless, rate of hydrogenation of either LA or AL is higher than the rate of dehydration of LA. This could be explained from the product distribution that gVL selectivity is four times higher than the AL selectivity even at a reaction temperature of 425 °C (Table 4).

The influence of H_2O on the hydrogenation activity of Ru is tested by using pure levulinic acid (Table 4). A very low LA conversion (~4%) with 100% selectivity towards α-AL is observed. Our results are in good correlation with Michel et al. who showed importance of H_2O in the LA hydrogenation activity of Ru catalysts [40].

The catalytic activity of Ru/HAP has also been examined using LA in methanol, LA in ethanol, and the results are compared with aqueous LA. The product distribution at various reaction temperatures using LA in CH_3OH at a GHSV = 2.616 mL g_{cat}^{-1} s^{-1} is presented in Table 5. The conversion of LA did not vary much upon increasing the reaction temperature from 275 to 425 °C. Interestingly the selectivity of gVL and angelica lactones are low in comparison to LA in H_2O feed. A new product i.e., methyl levulinate is obtained by esterification of LA with methanol. This indicates a decrease in overall hydrogenation activity of Ru in contrast to LA in H_2O. The recent reports explained the role and importance of H_2O in feed stream for the Ru/TiO_2 catalyst in the hydrogenation of LA to gVL [41,42]. Similar result is observed in the case of LA in C_2H_5OH, where in large excess of ethyl levulinate ca. 24% is formed (Table 5) even at 275 °C. Rate of esterification of LA with C_2H_5OH is too high when compared to the rate of methyl levulinate at high reaction temperatures. It is generally known that dehydration and

Table 5
Hydrogenation of levulinic acid in CH_3OH and C_2H_5OH over 2wt% Ru/HAP at different reaction temperatures and constant GHSV = 2.616 mL g_{cat}^{-1} s^{-1}.

Temperature(°C)	LA in CH_3OH (μmol g_{cat}^{-1} s^{-1})			LA in C_2H_5OH (μmol g_{cat}^{-1} s^{-1})		
	[a]r_{GVL}	[b]r_{AL}	[c]r_{ML}	[d]r_{GVL}	[b]r_{AL}	[e]r_{EL}
275	56.7	–	7.04	44.3	–	14.0
325	56.6	2.8	6.24	42.2	1.21	15.6
375	54.8	5.1	7.02	38.5	1.24	22.4
425	53.4	4.8	7.35	33.6	3.73	24.8

[a] rate of gamma-valerolactone using CH_3OH as solvent.
[b] rate of angelica lactones (includes both α- and β).
[c] rate of methyl levulinate.
[d] rate of gamma-valerolactone using C_2H_5OH as solvent.
[e] rate of ethyl levulinate.

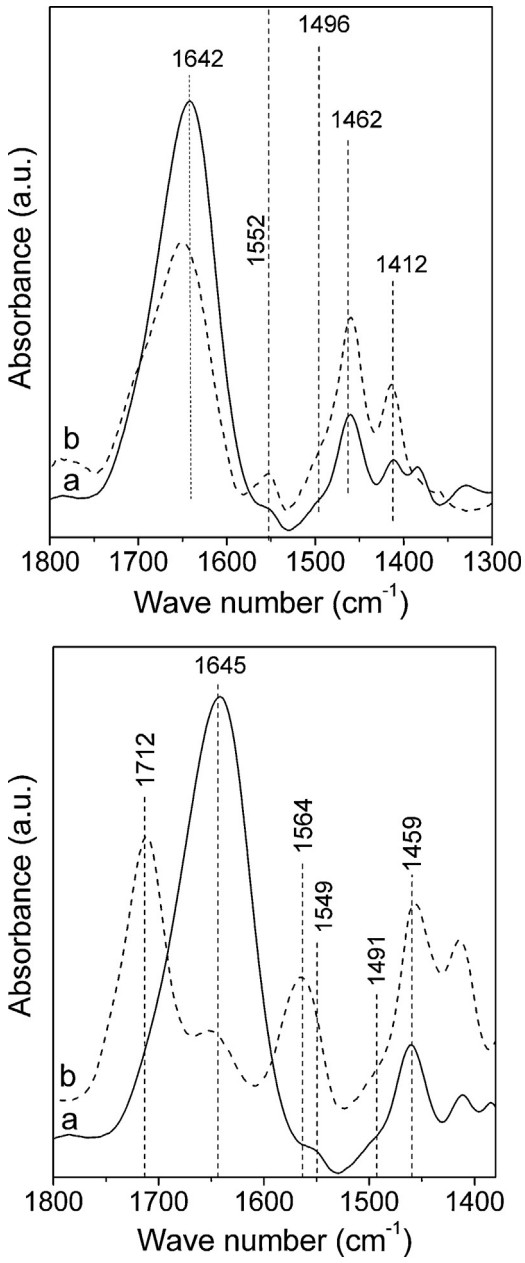

Fig. 6. FT-IR spectra of pyridine adsorbed (**a1**) 2wt%Ru/HAP; (**a2**) 2wt%Ru/TiO_2 and (**b1**) 2wt%Ru/HAP; (**b2**) 2wt%Ru/ SO_4^{2-}-HAP samples. The samples were successively treated priority to record the spectra; (i) the samples were reduced *in-situ* by heating in H_2/Ar flow (5 mL min^{-1}) at a ramping rate of 10 °C/min up to 450 °C/1 h. (ii) After cooling down to 150 °C the spectra were collected in the DRIFT mode. (iii) Subsequently the samples were exposed to steam at 275 °C and then flushed in N_2 (5 mL/min) for 30 min followed by recorded the spectra. (iv) In sequential step the samples were cooled to 180 °C and doses of pyridine injected and the spectra were recorded.

esterification reactions occur on acid sites present on the catalyst surface. Hence the reaction proceeds first by hydrogenation of LA to γ-hydroxyvaleric acid on metal particle followed by its dehydration on acid site to form gVL, as pure HAP showed neither dehydration nor hydrogenation activity. It should be mentioned here that none of these samples showed reforming activity in presence of either methanol or ethanol.

Hydrogenation activity of Ru is controlled by the reaction environment [43]. It has been reported that Ru based catalysts show higher LA hydrogenation activity in presence of H_2O [40]. Surprisingly when pure LA is subjected to Ru/HAP, 100% AL is observed. According to mechanism, LA conversion to gVL is required to have both metal and weak or moderate acidic sites to be present on the surface. In the absence of H_2O the reaction proceeds by esterification followed by hydrogenation of carbonyl group with subsequent intra molecular cyclisation yielding gVL. On the other hand in presence of H_2O the LA hydrogenation occurs followed by dehydration reaction. The activity of Ru/HAP is measured subjected to hydrogenation of aqueous levulinic acid for long period. The Ru/HAP exhibited consistent activity up to 48 h (SI). Hence it can be concluded that HAP could be a promising support for Ru in the synthesis of γ-valerolactone.

The reduced surface of metal/metal oxide upon exposure to H_2O at ≥275 °C; convert the coordinatively unsaturated species into hydroxyl groups by dissociative adsorption on the catalyst surface [44]. These hydroxyl groups possess both Bronsted and Lewis acidity, although they behave as basic –OH groups, because the bond with which they are coordinated to the metal cation is ionic. Such an effect is not observed in the FT-IR analysis of pyridine adsorbed Ru/HAP catalyst. For comparative analysis Ru/TiO_2 and Ru/HAP samples have been subjected to FT-IR analysis using pyridine as a probe and the spectra is reported in Fig. 6. The vibrational band that appeared at 1458 cm^{-1} in both Ru/TiO_2 and Ru/HAP is an indication of Lewis acid sites. Band at 1550 cm^{-1} is prominent in Ru/TiO_2 and a very weak signal in this region is found with Ru/HAP sample (Fig. 6a). The activity data on Ru/TiO_2 showed ~50% LA conversion with 42%, 48% and 10% selectivities of gVL, angelica lactone and pentanoic acid respectively. FT-IR analysis of the pyridine adsorbed spectra revealed the presence of highly populated Lewis acid sites and very weak Bronsted acid sites on the Ru/HAP surface. These results clearly demonstrated the role of surface hydroxyl groups as illustrated by Dumesic et al. [9,34].

The FT-IR spectra of Pyridine adsorbed on sulphated HAP sample (Fig. 6b) showed strong acid sites at 1455 cm^{-1} (Py M^{n+}) and a vibrational band due to (Py H^+) at 1552 cm^{-1}. A strong Fermi resonance appeared with Ru/SO_4^{2-}-HAP particularly at 1550 cm^{-1} region (Fig. 6b). However no shift in vibrational band at 1450 cm^{-1} is found in both Ru/HAP and Ru supported sulphated HAP. The band at 1550 cm^{-1} in Ru/HAP shifted to higher wave number compared to the band that appeared at 1565 cm^{-1} for the Ru/SO_4^{2-}-HAP. These results suggest enhanced Bronsted acidity on Ru supported on SO_4^{2-}-HAP whereas Ru/HAP showed Bronsted acid sites with weak acidity. The Ru supported on sulphated HAP is tested for LA hydrogenation at GHSV = 3.89 mL g^{-1} s^{-1} and the results are presented in Table 4. At a reaction temperature of 275 °C, LA conversion is low (44.5%), and α-AL is selectively (92.8%) formed with 4.2% gVL and 3% of pentanoic acid (PA).

Based on the activity data in conjunction with the FT-IR it can be concluded that strong Bronsted acid sites on Ru/SO_4^{2-}-HAP catalyze LA dehydration to α-AL selectively. We believe that surface metal site along with weak Bronsted sites are active for simultaneous hydrogenation and dehydration of levulinic acid to gVL. The Ru/HAP displayed angelica lactones only at high reaction temperatures. This probably could be explained by the influence of strong acid sites at high reaction temperatures as the TPD of NH_3 results indicated the shift in T_{max} to high temperatures.

5. Conclusions

The metal (M = Ni, Pt, Pd and Ru) supported on hydroxyapatite catalysts are active (at low temperature) for the hydrogenation of levulinic acid to γ-valerolactone. Ru/HAP showed better γ-valerolactone yield in H_2O compared to CH_3OH and C_2H_5OH. Ru/HAP exhibited superior activity although the Ru dispersion is lower than Pt/HAP and Pd/HAP catalysts. At high reaction temperatures, γ-valerolactone yield decreased slightly due to the formation

of angelica lactones. Presence of weak Bronsted and moderate Lewis acid sites is a possible reason for the high selectivity towards gVL as indicated by the FT-IR spectra of pyridine adsorbed Ru/HAP catalyst. Hydroxyapatite has been found to be a suitable support for metal Ru in the selective vapour phase hydrogenation of levulinic acid to γ-valerolactone. It has also been observed that sulphated HAP supported Ru showed lower LA conversion with high selectivity towards α-angelica lactone along with pentanoic acid.

Acknowledgements

One of the authors MS thank CSIR New Delhi, VV and GN thank RMIT Australia for fellowship.

Appendix A. Supplementary data

Supplementary data associated with this article can be found, in the online version, at http://dx.doi.org/10.1016/j.apcatb.2015.05.050

References

[1] D.M. Alonso, J.Q. Bond, J.A. Dumesic, Green Chem. 12 (2010) 1493–1513.
[2] A.C. Caputo, M. Palumbo, P.M. Pelagagge, F. Scacchia, Biomass Bioenergy 28 (2005) 35–51.
[3] D.M. Alonso, S.G. Wettstein, J.A. Dumesic, Chem. Soc. Rev. 41 (2012) 8075–8098.
[4] E. Taarning, C.M. Osmundsen, X. Yang, B. Voss, S.I. Andersen, C.H. Christensen, Energy Environ. Sci. 4 (2011) 793–804.
[5] F.M. Geilen, B.A. Engendahl, M. Holscher, J. Klankermayer, W. Leitner, Angew. Chem. Int. Ed. 49 (2010) 5510–5514.
[6] X. Du, L. He, S. Zhao, Y.L. Mei, Y. Cao, H.Y. He, K.N. Fan, Angew. Chem. Int. Ed. 50 (2011) 7815–7819.
[7] H.N. Pham, Y.J.P. Torres, J.C.S. Ruiz, D. Wang, J.A. Dumesic, A.K. Datye, Appl. Catal. A Gen. 397 (2011) 153–157.
[8] M. Chalid, H.J. Heeres, A.A. Broekhuis, J. Appl. Polym. Sci. 123 (2012) 3556–3564.
[9] J.Q. Bond, D.M. Alonso, R.M. West, J.A. Dumesic, Langmuir 26 (2010) 16291–16298.
[10] J.M. Tukacs, D. Kiraly, A. Stradi, G. Novodarszki, Z. Eke, G.D.T. Keglb, L.T. Mika, Green Chem. 14 (2012) 2057–2065.
[11] D. Fegyverneki, L. Orh, G. Lang, I.T. Horvath, Tetrahedron 66 (2010) 1078–1081.
[12] I.T. Horvath, H. Mehdi, V. Fabos, L. Boda, L.T. Mika, Green Chem. 10 (2008) 238–242.
[13] Y. Fukaya, Y. Lizuka, K. Sekieaka, H. Ohno, Green Chem. 9 (2007) 1155–1157.
[14] F. Joo, M.T. Beck, React. Kinet. Catal. Lett. 2 (1975) 257–263.
[15] H. Mehdi, V. Fabos, R. Tuba, A. Bodor, L.T. Mika, I.T. Horvath, Top. Catal. 48 (2008) 49–54.
[16] W. Luo, U. Deka, A.M. Beale, E.R.H. van Eck, B.M. Weckhuysen, J. Catal. 301 (2013) 175–186.
[17] L.C. Demailly, B.K. Ly, D.P. Minh, B. Tapin, C. Especel, F. Epron, A. Cabiac, E. Guillon, M. Besson, C. Pinel, ChemSusChem. 6 (2013) 2388–2395.
[18] P.P. Upare, J.M. Lee, D.W. Hwang, S.B. Halligudi, Y.K. Hwang, J.S. Chang, J. Ind. Eng. Chem. 17 (2011) 287–292.
[19] M. Sudhakar, M. Lakshmi Kantam, V.S. Jaya, R. Kishore, K.V. Ramanujachary, A. Venugopal, Catal. Commun. 50 (2014) 101–104.
[20] M. Zahmakıran, Y. Tonbulz, S.O. Zkar, Chem. Comm. 46 (2010) 4788–4790.
[21] J. -Paul Lange, R. Price, P.M. Ayoub, J. Louis, L. Petrus, L. Clarke, H. Gosselink, Angew. Chem. Int. Ed. 49 (2010) 4479–4483.
[22] A. Venugopal, M.S. Scurrell, Appl. Catal. A Gen. 245 (2003) 137–147.
[23] J.A.S. Bett, L.G. Christner, W.K. Hall, J. Am. Chem. Soc. 89 (1967) 5535–5541.
[24] M.P. Reddy, A. Venugopal, M. Subrahmanyam, Water Res. 41 (2007) 379–386.
[25] M.P. Reddy, A. Venugopal, M. Subrahmanyam, Appl. Catal. B 69 (2006) 164–170.
[26] S.G. Wettstein, J.Q. Bond, D.M. Alonso, H.N. Pham, A.K. Datye, J.A. Dumesic, Appl. Catal. B: Environ. 117–118 (2012) 321–329.
[27] W. Luo, U. Deka, A.M. Beale, E.R.H. van Eck, P.C.A. Bruijnincx, B.M. Weckhuysen, J. Catal. 301 (2013) 175–186.
[28] W. Luo, P.C.A. Bruijnincx, B.M. Weckhuysen, J. Catal. 320 (2014) 33–41.
[29] K. Yuliana Lugo-José, R. John Monnier, T. Christopher Williams, Appl. Catal. A: Gen. Appl. Catal. A: Gen. 469 (2014) 410–418.
[30] M. Grilc, B. Likozar, J. Levec Biomass Bioenergy 63 (2014) 300–312.
[31] M. Grilc, B. Likozar, J. Levec Appl. Catal. B: Environ. 150–151 (2014) 275–287.
[32] M. Grilc, G. Veryasov, B. Likozar, A. Jesihb, J. Levec, Appl. Catal. B: Environ. 163 (2015) 467–477.
[33] K. Kon, W. Onodera, K. Shimizu, Catal. Sci. Technol. 4 (2014) 3227–3234.
[34] J.Q. Bond, D. Wang, D.M. Alonso, J.A. Dumesic, J. Catal. 281 (2011) 290–299.
[35] M. Lakshmi Kantam, R. Sudarshan Reddy, P. Ujjwal, M. Sudhakar, A. Venugopal, K. Jeevaratnam, F. Figueras, C. Venkat Reddy, Y. Nishina, J. Mol. Catal. A 359 (2012) 1–7.
[36] R. Berthoud, P. Delichere, D. Gajana, W. Lukens, K. Pelzer, J.M. Basset, J.P. Candy, C. Copereta, J. Catal. 260 (2008) 387–391.
[37] P. Sangeetha, K. Shanthi, K.S. RamaRao, B. Viswanathan, P. Selvam, Appl. Catal. A Gen. 353 (2009) 160–165.
[38] H. Liu, G. Lu, Y. Guo, Y. Wang, Y. Guo, J. Colloid Interface Sci. 346 (2010) 486–493.
[39] E. Symianakis, S. Ladas, G.A. Evangelakis, Appl. Surf. Sci. 217 (2003) 239–249.
[40] J. Wu, Y. Shen, C. LiC, H. Wang, C. Geng, Z. Zhang, Catal. Comm. 6 (2005) 633–637.
[41] C. Michel, A.M. Zaff;ran, M. Matras-Michalska, J. Grams, P. Sautet, Chem. Commun. 50 (2014) 12450–12453.
[42] M. Chia, J.A. Dumesic, Chem. Commun. 47 (2011) 12233–12235.
[43] B.S. Akpa, C.D. Agostino, L.F. Gladden, K. Hindle, H. Manyar, J. McGregor, R. Li, M. Neurock, N. Sinha, E.H. Stitt, D. Weber, J.A. Zeitler, D.W. Rooney, J. Catal. 289 (2012) 30–41.
[44] G. Busca, Catal. Today 41 (1998) 191–206.